JCB Report

The nonhelical tail domain of keratin 14 promotes filament bundling and enhances the mechanical properties of keratin intermediate filaments in vitro

Olivier Bousquet,[1] Linglei Ma,[1] Soichiro Yamada,[2] Changhong Gu,[1] Toshihiro Idei,[3] Kenzo Takahashi,[4] Denis Wirtz,[2] and Pierre A. Coulombe[1]

[1]Department of Biological Chemistry, School of Medicine and [2]Department of Chemical Engineering, Johns Hopkins University, Baltimore, MD
[3]Department of Dermatology, Kyoto University Graduate School of Medicine, Kyoto, Japan
[4]Department of Dermatology, Gunma University School of Medicine, Maebashi, Japan

Downloaded from http://rupress.org/jcb/article-pdf/155/5/747/1300632/jcb1555747.pdf by guest on 20 June 2021

Keratin filaments arise from the copolymerization of type I and II sequences, and form a pancytoplasmic network that provides vital mechanical support to epithelial cells. Keratins 5 and 14 are expressed as a pair in basal cells of stratified epithelia, where they occur as bundled arrays of filaments. In vitro, bundles of K5–K14 filaments can be induced in the absence of cross-linkers, and exhibit enhanced resistance to mechanical strain. This property is not exhibited by copolymers of K5 and tailless K14, in which the nonhelical tail domain has been removed, or copolymers of K5 and K19, a type I keratin featuring a short tail domain. The purified K14 tail domain binds keratin filaments in vitro with specificity (kD ~2 μM). When transiently expressed in cultured cells, the K14 tail domain associates with endogenous keratin filaments. Utilization of the K14 tail domain as a bait in a yeast two-hybrid screen pulls out type I keratin sequences from a skin cDNA library. These data suggest that the tail domain of K14 contributes to the ability of K5–K14 filaments to self-organize into large bundles showing enhanced mechanical resilience in vitro.

Introduction

Keratins (40–70 kD) are the major structural proteins of epithelial cells, where they occur as intermediate-sized filaments in the cytoplasm. The >49 functional keratin-encoding genes in the human genome (Hesse et al., 2001) occur as two major types, I and II. Keratin filaments are built from lateral and longitudinal interactions involving heterodimers, and most keratin genes are regulated in a pairwise and differentiation-related fashion within epithelia. A major function of keratin intermediate filaments (IFs)* is to endow epithelial cells with mechanical resilience. Mutations in keratin proteins result in fragility states whereby the cell type(s) affected ruptures when subjected to trauma (Fuchs and Cleveland, 1998). Bundles represent the preferential form of keratin filaments in complex epithelia. Whether they are examined in situ or in primary culture, basal keratinocytes of the skin exhibit loosely packed bundles of keratin filaments in their cytoplasm. However, there is no known cross-linking activity that is keratin filament–specific in the cytoplasm of these and many other epithelial cells in which keratin occurs as bundled arrays (Coulombe et al., 2000).

In vitro, keratin filaments can be induced to form large bundles after minor changes to the buffer conditions, in the absence of exogenous proteins. As expected, this significantly enhances the mechanical resilience of keratin gels (Ma et al., 2001). Along with other data (Coulombe et al., 2000), this suggests that keratin IFs can modulate their organization and mechanical properties though self-interaction. Here we provide evidence that the nonhelical tail domain of K14, the predominant type I keratin in basal cells of skin epithelia, binds keratin filaments in vitro and ex vivo, and contributes to the remarkable properties of keratin filaments.

Address correspondence to Pierre A. Coulombe, Dept. of Biological Chemistry, Johns Hopkins University School of Medicine, 725 N. Wolfe St., Baltimore, MD 21205. Tel.: (410) 614-0510. Fax: (410) 614-0510. E-mail: coulombe@jhmi.edu

O. Bousquet and L. Ma contributed equally to this work.

*Abbreviations used in this paper: His, histidine; IF, intermediate filament.

Key words: keratin; intermediate filament; tail domain; rheology; cross-linker

© The Rockefeller University Press, 0021-9525/2001/11/747/7 $5.00

Results and discussion

The nonhelical tail domain contributes to the mechanical properties of cross-linked keratin gels

Polymerization of K5–K14 in low ionic strength buffer adjusted at pH 7.0, or at pH 7.4 with 10–20 mM NaCl added, results in the formation of large bundles of filaments that can be seen using DIC light microscopy. Rheological assays show that suspensions of bundled keratin filaments maintain their elasticity and solid-like character even when subjected to large deformations. These data (Ma et al., 2001) imply that stable filament–filament interactions, which depend upon cis-acting elements, occur under these conditions.

There is evidence suggesting that the COOH-terminal tail domain of cytoplasmic IF proteins may influence filament–filament interactions (Herrmann and Aebi, 1998). Moreover, the tail domain of K14 is not required for efficient copolymerization with K5 (Coulombe et al., 1990; Wilson et al., 1992). We compared the properties of wt K5–K14 and K5–K14ΔT assemblies at pH 7.0 to assess the role of K14's tail domain toward bundling. Whereas wt K5–K14 displays the texture of a gel under this condition, the K5–K14ΔT polymer (Fig. 1 A) flows like a liquid. In a high-speed pelleting assay designed to measure polymerization efficiency, >95% of both the wt K5–K14 and K5–K14ΔT protein pools are retrieved in the pellet (Fig. 1 B). In a low-speed pelletting assay devised to assess the formation of cross-linked networks (Pollard and Cooper, 1982), nearly all the wt K5–K14 proteins end up in the pellet, compared with only ~20% for K5–K14ΔT. DIC light microscopy confirms the presence of extensive bundling in the wt K5–K14 sample, whereas few bundles can be seen for K5–K14ΔT (unpublished data).

In rheological studies, the wt K5–K14 and K5–K14ΔT assemblies produced at pH 7.0 both display properties typical of viscoelastic solids when subjected to small deformations (Fig. 1 C). K5–K14ΔT displays a slightly larger phase shift compared with wt K5–K14 (12° vs. 6°, respectively), indicating subtle differences in the solid-like character of these samples when in the linear regime. However, significant differences are seen when these samples are subjected to larger deformations. Whereas wt K5–K14 maintains its elasticity up to deformations exceeding 300% and shows a "bump" characteristic of strain hardening before softening, K5–K14ΔT begins to soften at 10% strain and shows comparatively less strain hardening before yielding (Fig. 1 C). Strain hardening can be captured in real time through a faster-than-linear increase of the shear stress $\sigma(t)$ when it is monitored continuously while a fixed oscillatory deformation γ (of amplitude 100%) is applied to the sample (Ma et al., 2001). In pH 7.0 assembly buffer, wt K5–K14 displays significant strain hardening (Fig. 1 D). In contrast, the K5–K14ΔT polymer shows little of this behavior (Fig. 1 D).

The K14ΔT protein we used has a 12-amino-acid-long epitope tag at its COOH terminus (Albers and Fuchs, 1987). To rule out that its rheological properties stem in part from this short tag, we repeated these studies with wt K5–K19 polymer (Fradette et al., 1998). K19 features a short tail domain (13 amino acids) and is coexpressed with K5 in a subset of progenitor basal cells in the skin (Stasiak et al., 1989). Rheological studies show that K5–K19 behaves like a weak viscoelastic solid when subjected to small deformations at pH 7.0. However, as is the case for K5–K14ΔT (Fig. 1 B), the K5–K19 polymer rapidly softens when subjected to progressively larger deformations. At 200% strain amplitude, for instance, the wt K5–K14 and K5–K19 assembled at 0.2 mg/ml (4 μm) exhibit elastic moduli G′ of 38 ± 7 and 4.2 ± 0.2 dynes/cm^2, respectively. Interestingly, immunoelectron microscopy studies involving human skin

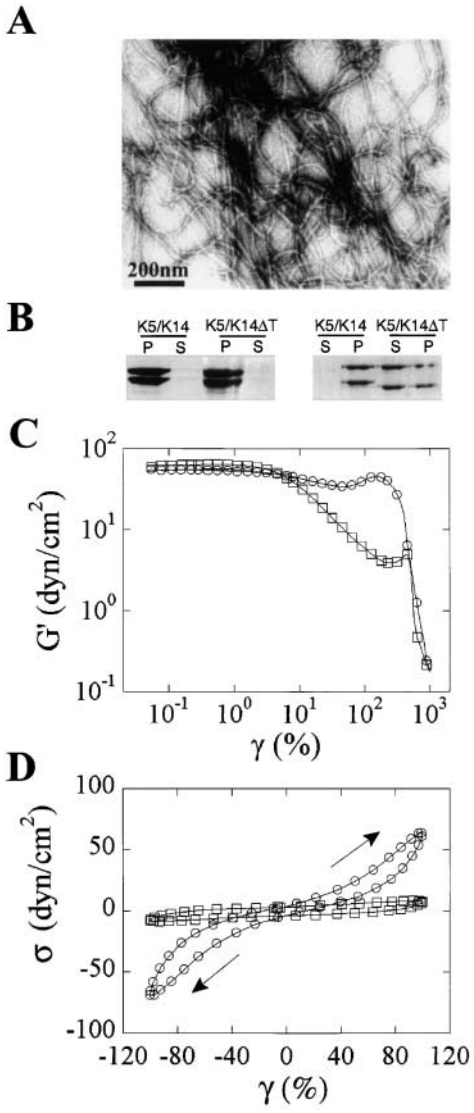

Figure 1. **Rheological assessment of bulk properties of keratin polymers.** All studies were conducted in low–ionic strength Tris-HCl buffer at pH 7.0. (A) Electron micrograph of K5–K14ΔT polymer subjected to negative staining. (B) Sedimentation assays for wt K5–K14 and K5–K14ΔT polymers spun at 150,000 × *g* (left) and 8,200 × *g* (right). P, pellet; S, supernatant. See Materials and methods for details. (C) Strain dependence of elastic modulus G′ of the wt K5–K14 (○) and K5–K14ΔT (□) polymers. These findings are highly reproducible between experiments. γ, strain amplitude. (D) Time-resolved stress versus strain relationship experiment was conducted at a 100% strain amplitude. Wild-type K5–K14 (○); K5–K14ΔT (□). The arrows depict the direction of the oscillations of the strain-inducing plate. Data corresponding to the first cycle of shear are shown (Ma et al., 2001).

Downloaded from http://rupress.org/jcb/article-pdf/155/5/747/1300632/jcb1555747.pdf by guest on 20 June 2021

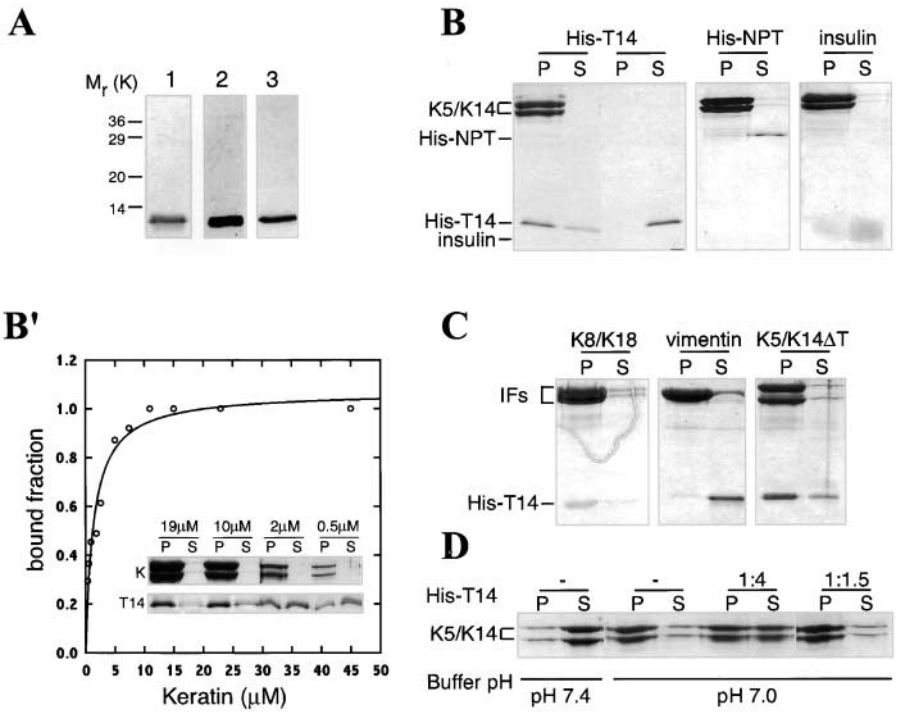

Figure 2. **The purified recombinant K14 tail domain binds keratin filaments in vitro.** (A) Electrophoretic analysis of purified recombinant His-T14. (Lane 1) Coomassie blue staining. (Lanes 2 and 3) Western immunoblots probed with antibodies directed against the His tag (2) and the K14 tail domain (3). (B) Cosedimentation of His-T14 with wt K5–K14 filaments in Tris-HCl buffer at pH 7.4 (standard conditions). His-T14 was mixed in a 1:1 molar ratio with preformed filaments (10 μM; left) or not (right). As controls, His-NPT or insulin do not cosediment with wt K5–K14 under the same conditions. (B′) Binding curve defining the interaction between wt K5–K14 (X axis) and His-T14 (fixed concentration). The Y axis corresponds to the fraction of His-T14 bound. The inset shows some of the cosedimentation data (K, K5–K14; T14, His-T14). Nonlinear regression analysis indicates that His-T14 binds keratin IFs with an apparent kD of 2 μM. (C) Assessment of His-T14 binding to other IF polymers. His-T14 binds reconstituted K8–K18 filaments (10 μM) and K5–K14ΔT filaments (10 μM) but not vimentin filaments (10 μM). (D) Impact of adding purified His-T14 on the low pH-induced bundling of wt K5–K14 filaments (10 μM), as assessed by a low-speed centrifugation assay. P, pellet; S, supernatant. Under such conditions, the bulk of K5-K14 is retrieved in the supernatant when assembled at pH 7.4, and in the pellet when assembled at pH 7.0. Addition of His-T14 at a 1:4 stoichiometry partially inhibits the low pH induced sedimentation. Paradoxically, adding His-T14 at a higher stoichiometry (1:1.5) has no effect.

epithelia showed that K5–K19-rich basal cells exhibit a looser keratin network than K5–K14-rich basal cells (Dr. Lucie Germain, personal communication). The data we report here suggest that although the nonhelical tail domain of K14 is dispensable for 10-nm filament assembly, it contributes to the intrinsic potential of K5–K14 for interaction with self, which enhances its ability to withstand large deformations.

The purified K14 tail domain binds to keratin filaments in vitro

To assess whether the short nonhelical tail domain of K14 (~50 residues) can interact directly with keratin filaments, we added an NH_2-terminal histidine (His) tag to facilitate its purification. Purified His-T14 migrates with a mass of ~7 kD on SDS-PAGE, reacts with antibodies directed against the His tag and the K14 COOH terminus (Fig. 2 A), and behaves as a monomer with an extended shape in solution (unpublished data). His-T14 cosediments with wt K5–K14 filaments produced under standard buffer conditions at pH 7.4 (Fig. 2, B and B′, kD ~2 μM). In contrast, His-NPT (control for His tag) and insulin (size control) do not cosediment (Fig. 2 B), establishing specificity. His-T14 also cosediments with K8–K18 filaments and K5–K14ΔT filaments (Fig. 2 C), but not with vimentin filaments (Fig. 2 C) or F-actin (unpublished data). Therefore, the tail domain of K14 binds directly to determinant(s) shared between K5–K14 and K8–K18 filaments.

The outcome of the binding studies predicts that an excess of purified His-T14 should inhibit the gelation of keratin filaments induced by lower pH or added salt. We tested His-T14:keratin stoichiometries ranging from 1:8 to 3:1 (Fig. 2 B′). Bundle formation was scored through a low-speed centrifugation assay (10,000 × *g*, 20 min). In the absence of His-T14 and at pH 7.0, virtually all of the K5–K14 pool is retrieved in the pellet fraction (Fig. 2 D). Adding His-T14 at low stoichiometry (i.e., 1:4) caused a redistribution of wt K5–K14 to the supernatant (Fig. 2 D). This effect was not seen at the higher concentrations of His-T14 tested (Fig. 2 D). The reasons for this observation are unclear. These studies show that addition of the His-T14 can partially inhibit the gelation of wt K5–K14 induced by low pH under some conditions.

The K14 tail domain associates with keratin filaments in epithelial cells in culture

We performed transient transfection assays with constructs in which the K14 tail domain is fused to a myc epitope tag. In PtK2 cells, an epithelial cell line that displays keratin and vimentin IF networks, Myc-T14 is detected in the cytoplasm, where it occurs as a filamentous pattern, as well as in the nucleus, where it does not exhibit any pattern (Fig. 3, A and B). Double-immunofluorescence staining shows that in the cytoplasm, the signal for myc-T14 colocalizes with K8–K18 filaments to a significant extent (Fig. 3, A′, A″, B′, and B″), but not with vimentin IFs (unpublished data). The best instances of colocalization involved bundles of keratin filaments whose shape and organization are reminiscent of stress fibers. Dual immunostaining of untransfected PtK2 cells

Downloaded from http://rupress.org/jcb/article-pdf/155/5/747/1300632/jcb1555747.pdf by guest on 20 June 2021

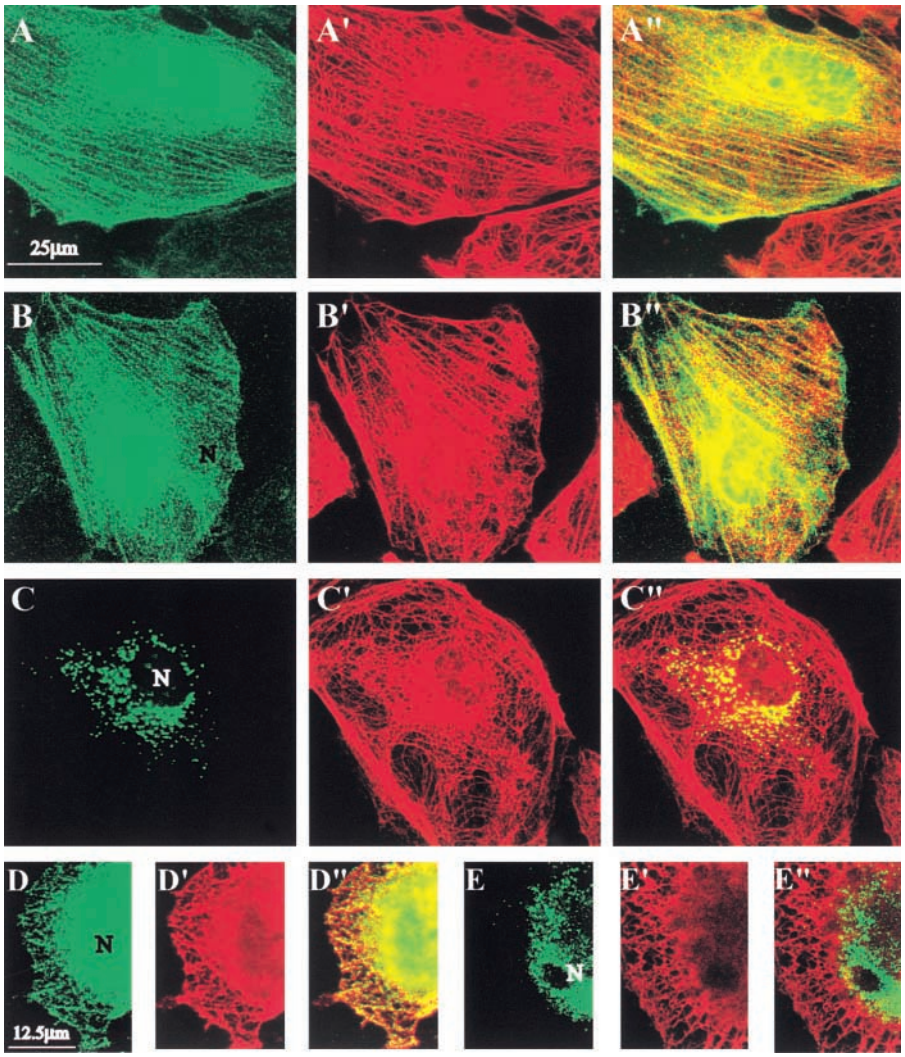

Figure 3. **Transient expression of Myc-T14 or controls in various cell lines.** (A–A′′ and B–B′′) Expression of myc-T14 in Ptk2 cells. Myc immunostaining (A and B) localizes to the nucleus and the cytoplasm, where it occurs in a fibrous pattern that coaligns to a significant extent with the endogenous keratin filament network (A′ and B′), as shown in the merged images (A′′ and B′′). (C–C′′) Expression of myc-PTE1 in Ptk2 cells. Myc immunostaining (C) shows a puncate pattern in the cytoplasm that is clearly distinct from the endogenous keratin filament network (C′ and C′′). (D–D′′ and E–E′′) Coexpression of K5, K14, along with either myc-T14 (D–D′′) or myc-PTE1 (E–E′′) in BHK-21 cells. Myc-T14 distributes to both the nucleus (N) and the cytoplasm; in this latter instance, it colocalizes with keratin polymers (D′ and D′′). In contrast, the localization of Myc-PTE1 (E) and keratin polymers (E′) are clearly distinct (E′′).

for F-actin and K8–K18 shows that the two types of filaments are closely apposed in a significant fraction of cells, indicating that this phenomenon is not a function of myc-T14 expression (unpublished data). Myc-T14 may thus show a greater affinity for a specific subset of keratin filaments, or weakly promote the formation of straight K8–K18 bundles. Alternatively, this observation may simply stem from the sensitivity of the assay. Transfected myc-PTE1, used as a control, exhibits a punctate cytoplasmic pattern that is independent from keratin filaments (Fig. 3, C–C″). Similar results were obtained in mouse 308 cells, a K5–K14-expressing skin keratinocyte line (unpublished data).

We next performed triple transfection assays in BHK-21 fibroblasts, a cell line that does not contain any keratin filaments. In cells coexpressing K5, K14, and Myc-T14, there is a significant spatial correspondence between the signals for myc and for K14 (Fig.3, D–D″). Again, a significant fraction of the myc signal is localized to the nucleus (Fig. 3 A). In contrast, the transfected myc-PTE1 localizes both to the nucleus and cytoplasm, but is clearly distinct from K5–K14 filaments (Fig. 3, E–E″). We conclude that the nonhelical tail domain of K14 can specifically bind keratin filaments in the cytoplasm of various cell lines in culture.

The K14 tail domain interacts with type I keratin sequences in a yeast two-hybrid screen

In an effort to isolate tail domain binding proteins, the COOH termini of both human K14 and K16 were used as baits in a yeast two-hybrid screen involving a human cDNA library made from a squamous cell carcinoma of the leg. Among 2,000,000 cfus screened with the K14 tail domain, 121 scored positive for both growth on His-minus medium and *lacZ* expression. Among the 40 clones sequenced, 32 (80%) corresponded to type I keratin sequences, and an additional 2 clones corresponded to a keratin-related sequence. The 5′ boundary of all the interacting type I keratin clones is given in Fig. 4 A. These findings can be interpreted in two ways. First, the K14 tail domain binds multiple sites along type I keratin sequences (Fig. 4 B). Some of these sites would be shared among them (i.e., linker L12), and others potentially unique (e.g., the head domain of K14). Second, the tail domain binds a restricted number of sites, perhaps a single one, located within the COOH-terminal half of the rod domain of many type I sequences (Fig. 4, A and B). In this case, the heterogeneity observed at the 5′ end would reflect the manner with which the reverse transcriptase operated while making the library. Of note, all type I sequences contained at least coil 2 from the rod, and no type II keratin

Downloaded from http://rupress.org/jcb/article-pdf/155/5/747/1300632/jcb1555747.pdf by guest on 20 June 2021

A

Interacting Sequence	No. Clones	NH_2-terminal Boundary	Subdomain
K9	1	Asp 339	Coil 2A
	1	Gln 350	Coil 2A
K14	1	Gly 70	Head
	1	Ser 78	Head
	2	Gly 85	Head
	3	Gly 109	Head
	1	Glu 115	Coil 1A
	2	Ala 193	Coil 1B
	5	Asn 209	Coil 1B
	4	Ala 233	Coil 1B
K15	2	Gly 83	Head
K16	1	Asn 271	L12
	1	Val 272	L12
K17	2	Ala 86	Coil 1A
	1	Glu 240	L12
	1	Asp 242	L12
	1	Ala 243	L12

B

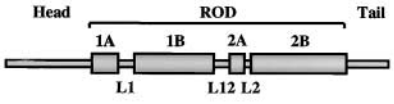

C

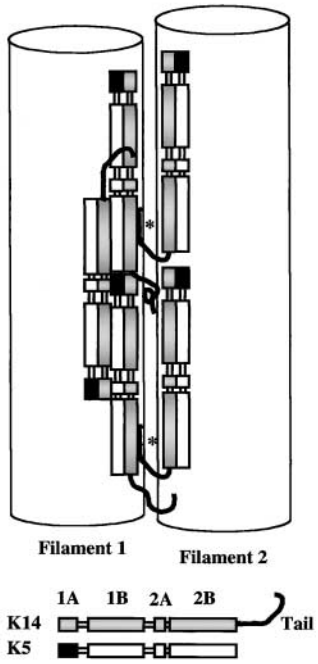

Figure 4. **Outcome of yeast two-hybrid screen and model for tail domain-mediated bundling.** (A) List of keratin sequences found to interact with the K14 tail domain in a yeast two-hybrid screen. All are type I keratins. The NH_2-terminal boundary of the individual clones, and the domain to which it maps to (B), are indicated. Full-length human K14 exhibits 472 amino acid residues. (B) Schematic depicting the secondary structure of type I keratin proteins. The central rod domain is dominated by α-helical subsegments (1A, 1B, 2A, and 2B) separated by short linker regions (L1, L12, and L2). The rod is flanked by nonhelical head and tail domains at the NH_2- and COOH-termini. (C) Modeling the interaction mediated by the K14 tail domain between two closely apposed keratin filaments. Coiled-coil heterodimers involving K5 and K14 are depicted near the filament-filament interface. For the sake of clarity, the nonhelical head domains of K5 and K14 and the tail domain of K5 are omitted, whereas the subdomain 1A of K5 is shown in black. An antiparallel tetramer (Herrmann and Aebi, 1998) is shown in filament 1. It should be noted that, on average, mature cytoplasmic IFs are comprised of 16 dimers in cross-section, that the coiled-coil central rod domain is 42–44 nm long, whereas the filaments themselves are 10–12 nm wide (Herrmann and Aebi, 1998). Individual elements are therefore not drawn to scale in this schematic. On average, 16 copies of the K14 tail domain should be present per 44–50-nm filament length. We postulate that a subset of these copies of the K14 tail domain are surface-exposed and engaged in a direct interaction with type I keratins in subunits from a closely apposed neighboring filament (*). These interactions would assist in the process of keratin filament bundling. The portion of the ~50 residue–long K14 tail domain mediating those interactions is unknown, but steric considerations along with lack of sequence homology with K16 suggest that it should reside within the distal half of the sequence. Reversible changes in the balance of charges (i.e., through phosphorylation) and other factors (i.e., associated proteins) are postulated to influence the stability of filament–filament interactions mediated by the exposed tail domains, and hence modulate self-induced bundling.

clones were pulled out. Among 3,500,000 cfus screened with the K16 tail domain, 581 scored positive. Among 143 clones that were sequenced, 132 encoded elongation factor 1 γ, and none encoded a keratin. The complete results of this screen will be published elsewhere. Meanwhile, these studies provide genetic evidence that K14's tail domain, but not K16's, can bind sequence determinant(s) shared by several type I keratins. These findings are interesting given the functional differences observed between K14 and K16 in the context of a protein replacement study in transgenic mouse skin (Paladini and Coulombe, 1999; Wawersik and Coulombe, 2000). These differences are, in part, due to the COOH-terminal 105 amino acids in these two homologous type I keratins. We have rheological evidence that suspensions of K5–K16 filaments are mechanically weaker than K5–K14 ones when prepared and tested under bundling-promoting conditions (unpublished data).

Defining a role for the nonhelical tail domain of keratins

The properties of the nonhelical tail domain of cytoplasmic IF proteins have been studied through mutagenesis. The consensus that emerged is that the tail domain contributes to the lateral growth and stability of filaments, and influences filament–filament interactions (Herrmann and Aebi, 1998). The tail domain of many type I keratins is not required for complete copolymerization with a type II keratin (Albers and Fuchs, 1987; Coulombe et al., 1990; Hatzfeld and Weber, 1990; Lu and Lane, 1990; Bader et al., 1991; Wilson et al., 1992). Limited proteolysis studies in vitro (Herrmann and Aebi, 1998) and accessibility to kinases in vivo (Omary et al., 1998) suggest that the tail domain of IF proteins is exposed at the filament surface. Extensive bundling of K5–K14 filaments in vitro can be promoted by small changes in the assembly buffer conditions (Ma et al., 2001). Here we show that this depends, in part, on the presence of the tail domain of K14. We provide biochemical and genetic evidence that the isolated tail domain behaves like a keratin binding protein, with an affinity comparable to that of most F-actin cross-linkers (Matsudaira, 1994). We propose a model (Fig. 4 C) in which the nonhelical tail domain of K14 (and possibly other keratins) contributes to the ability of keratin filaments to self-organize into bundles. Such interactions are postulated to assist in keratin organization and function in vivo. In support of this model, a frameshift mutation resulting in the loss of the COOH-terminal 21 residues in K1 was recently implicated in a failure of keratin filaments to bundle in differentiating epidermal keratinocytes, giving rise to a rare variant of epidermolytic hyperkeratosis (Sprecher et al., 2001).

The binding site(s) for the K14 tail domain on the keratin polymer is displayed by K5–K14, K5–K14ΔT, and K8–K18 filaments, and may be shared by several type I keratins (as suggested by the yeast two-hybrid screen). Electrostatic forces may well play a role in these interactions, as filament–filament contacts can be modulated by changes in pH and in salt conditions. Filaggrin, a known keratin cross-linker, binds keratin filaments via electrostatic interactions (Mack et al., 1993). Likewise, the 50-residue-long IF binding motif

Downloaded from http://rupress.org/jcb/article-pdf/155/5/747/1300632/jcb1555747.pdf by guest on 20 June 2021

contained within the tail domain of plectin is rich in basic residues (Nikolic et al., 1996). Given the estimate of ~700 keratin monomers per μm of filament length (Herrmann and Aebi, 1998), only a subset of polymer-bound tail domains need be exposed and involved in these interactions to account for a filament cross-bridging effect (Fig. 4 C). Additional studies are needed to define the binding sites and mechanism(s) involved, determine whether this applies to other keratin polymers, and assess the importance of this phenomenon for the mechanical scaffolding function of keratin polymers in vivo.

Materials and methods

Construction of fusion cDNAs

Preparation of His fusion proteins. For expression in *Escherichia coli*, the human K14 tail coding sequence (Marchuk et al., 1984) was subcloned into a bacterial expression vector, pT7–6 × His (Geisbrecht et al., 1999). The NH_2 terminus of the resulting fusion protein is MGSSHHHHHHSSGLVPRGSHMASGQSTM^{427}S, where the tag is underlined and ^{427}S corresponds to residue 427 in K14. His-NPT, used as a control, features the neomycin phosphotransferase sequence (GenBank/EMBL/DDB accession no. AF335419; MW 29.2 kD).

Preparation of Myc fusion proteins. For expression in mammalian cells, the K14 tail sequence was transferred to vector pcDNA3-Nmyc (Jones et al., 1999), which has a CMV promoter and a polyadenylation signal. The NH_2 terminus of the resulting fusion proteins is MAEQKLISEEDLLGSGSTM^{427}S, where the tag is underlined and ^{427}S correspond to the first residue of K14's tail domain. Myc-PTE1, which codes for a myc fusion to acyl-CoA thioesterase (Jones et al., 1999), was used as a control.

Production, expression, and purification of recombinant proteins

Plasmids pET-K5, pET-K14 (Coulombe and Fuchs, 1990), pET-K14ΔT (Coulombe et al., 1990), and pET-K19 (Fradette et al., 1998) were used to generate recombinant human proteins. For His-tagged proteins, the plasmids pET-His-T14 and pET-His-NPT were transformed into *E. coli* strain BL21 (DE3), and protein purification was done using a nickel column (Novagen). Routine electrophoretic assays were used to assess protein size, purity, and identity.

Filament assembly and analysis

Keratin IFs (0.5 or 1 mg/ml) were reconstituted by serial dialysis starting from type I–type II heterotypic complexes (Ma et al., 2001) using the following three buffers at room temperature: (a) 9 M urea, 25 mM Tris-HCl, pH 7.4, 25 mM β-ME for 4 h; (b) 2 M urea, 5 mM Tris-HCl, pH 7.4, 5 mM β-ME, for 1 h; and (c) 5 mM Tris-HCl, 5 mM β-ME, for >12 h (overnight). The pH of the last buffer was adjusted at values of 7.4 or 7.0, depending on the experiment. The physical state of the polymer and polymerization efficiency were assessed as described (Ma et al., 2001). Filament morphology was examined by negative staining (1% uranyl acetate) and electron microscopy (Philips CM120, Germany). Sampling was restricted to regions of the sample where individual filaments could be seen. Larger polymer structures (i.e., bundles) were examined using DIC light microscopy (Eclipse; Nikon). Bundling was assessed by subjecting the assemblies to low-speed centrifugation (8,200 × *g* for 20 min) (Pollard and Cooper, 1982) followed by SDS-PAGE. Human recombinant vimentin was assembled as described (Herrmann and Aebi, 1998). Purified actin and protocols were provided by Enrique de la Cruz (Yale University, New Haven, CT). For copelletting assays, 50 μl of assembled keratin (10 μM), vimentin (10 μM), and actin filaments (5 μM) were mixed with either His-T14, His-NPT (Geisbrecht et al., 1999), insulin (Sigma-Aldrich), or vinculin's tail domain, a gift from Dr. Susan Craig (Johns Hopkins University, Baltimore, MD). After 2 h, the mixtures were centrifuged at 150,000 × *g* for 30 min, and the pellet and supernatant fractions were analyzed by SDS-PAGE (Ma et al., 2001).

Rheological studies

All measurements (Coulombe et al., 2000) were obtained using a strain-controlled 50-mm cone-and-plate ARES 100 rheometer (Rheometrics, Inc.) as described (Ma et al., 2001). The linear equilibrium values of the elastic modulus G′ (ω) and loss (viscous) modulus G″(ω) of the suspensions were measured by setting oscillatory strain amplitude at $\gamma = 1\%$ and sweeping from low to high frequency ω. Strain-dependent viscoelastic moduli were measured by subjecting polymers to three cycles of deformation of increasing amplitude at 1 rad/sec^{-1}; G′ and G″ were computed from the maximum magnitude of the measured stress. To assess strain hardening, we conducted assays in which the stress was continuously monitored as eight cycles of oscillatory shear deformation were applied (Ma et al., 2001). These studies were repeated three times using independent protein preparations.

Yeast two-hybrid screen

PCR products corresponding to the human K14 tail domain, starting at ^{425}His (Marchuk et al., 1984), and the K16 tail domain, starting at ^{426}Ser (Paladini et al., 1995), were fused in frame to the GAL4 DNA binding domain in the yeast expression vector pAS2–1 (ClONTECH Laboratories, Inc.). For library screening, the *Saccaromyces cerevisiae* strain Y190 was transformed with AS-T14 or AS-T16. Single colonies were selected after growth in synthetic minimal carbon source (2% sucrose) medium lacking Trp, grown, and retransformed with a human skin cDNA library fused in GAL4 activator domain in pACT2 by a PEG-based method. This library was constructed from poly(A) mRNAs extracted from a squamous cell carcinoma including adjacent normal tissue. mRNA priming for reverse transcription was done using random hexamers, and products of 0.5–2.0-kb size were used to make the library. Transformed yeast cells were plated on SC medium lacking Trp, Leu, and His in the presence of 25 mM 3-amino-1, 2, 4-triazole, incubated at 30°C for 7 d. Growing colonies (His+) were subjected to β-galactosidase assay. Plasmids harboring cDNA were recovered from positive colonies and sequenced. As negative controls, AS-T14 and AS-T16 were tested for their interaction with K5 or K6 protein.

Cell lines, transfections, and immunological reagents

Cell lines were maintained as recommended by their sources: PtK2 (kidney epithelium of the rat kangaroo; American Type Culture Collection); 308 (mouse epidermal keratinocytes), a gift of Dr. Stuart Yuspa (National Cancer Institute, Bethesda, MD); and BHK-21 (baby hamster kidney fibroblasts; American Type Culture Collection). Transient transfections were performed using polyethylenimine (Sigma-Aldrich) as described (Boussif et al., 1995). At 24 or 48 h posttransfection, cells were fixed with 3.0% paraformaldehyde for 15 min, extracted with 0.01% Triton-X in PBS buffer for 5 min, and processed for indirect immunofluorescence. We used rabbit polyclonal antisera against K18 and K14, obtained from E. Fuchs (University of Chicago, Chicago, IL); mouse monoclonals against vimentin (V9; Sigma-Aldrich); the myc epitope (American Type Culture Collection) K14, a gift from Dr. Irene Leigh (Imperial Cancer Research Fund, London, UK), and K8–K18, a gift from Dr. Bishr Omary (Stanford university, Stanford, CA); and chicken polyclonal against K14 (Wawersik and Coulombe, 2000). For immunofluorescence microscopy, rhodamine- or FITC-conjugated goat anti–mouse or anti–rabbit secondary antibodies were used (Kirkegaard and Perry Labs). For Western blotting, we used enhanced chemiluminescence (Amersham Pharmacia Biotech) or alkaline phosphatase (Bio-Rad Laboratories) detection.

We thank Ms. Kelsie Bernot and Dr. Brian Geisbrecht for their generous help, and Drs. Steve Gould and Susan Craig (Johns Hopkins University), Stuart Yuspa, Enrique De La Cruz, Elaine Fuchs, Irene Leigh, and M. Bishr Omary for providing reagents.

These studies were supported by National Institutes of Health grants AR44232 and AR42047 to P.A. Coulombe, and National Science Foundation Grants CTS9812624 and DB19729358 to D. Wirtz.

Submitted: 16 April 2001
Revised: 8 October 2001
Accepted: 9 October 2001

References

Albers, K., and E. Fuchs. 1987. The expression of mutant epidermal keratin cDNAs transfected in simple epithelial and squamous cell carcinoma lines. *J. Cell Biol.* 105:791–806.

Bader, B.L., T.M. Magin, M. Freudenmann, S. Stumpp, and W.W. Franke. 1991. Intermediate filaments formed de novo from tailless cytokeratins in the cytoplasm and in the nucleus. *J. Cell Biol.* 115:1293–1307.

Boussif, O., Lezoualc'h, F., Zanta, M.A., Mergny, M.D., Scherman, D., Demeneix, B., Behr, J.P. 1995. A versatile vector for gene and oligonucleotide

Downloaded from http://rupress.org/jcb/article-pdf/155/5/747/1300632/jcb1555747.pdf by guest on 20 June 2021

transfer into cells in culture and in vivo: polyethylenimine. *Proc. Natl. Acad. Sci. USA.* 92:7297–7301.

Coulombe, P.A., and E. Fuchs. 1990. Elucidating the early stages of keratin filament assembly. *J. Cell Biol.* 111:153–169.

Coulombe, P.A., Y.M. Chan, K. Albers, and E. Fuchs. 1990. Deletions in epidermal keratins leading to alterations in filament organization in vivo and in intermediate filament assembly in vitro. *J. Cell Biol.* 111:3049–3064.

Coulombe, P.A., O. Bousquet, L. Ma, S. Yamada, and D. Wirtz. 2000. The "ins" and "outs" of intermediate filament organization. *Trends Cell Biol.* 10:420–428.

Fradette, J., L. Germain, P. Sessaiah, and P.A. Coulombe. 1998. The type I keratin 19 possesses distinct and context-dependent assembly properties. *J. Biol. Chem.* 273:35166–35184.

Fuchs, E., and D.W. Cleveland. 1998. A structural scaffolding of intermediate filaments in health and disease. *Science.* 279:514–519.

Geisbrecht, B.V., D. Zhang, H. Schulz, and S.J. Gould. 1999. Characterization of PECI, a novel monofunctional Delta(3), Delta(2)-enoyl-CoA isomerase of mammalian peroxisomes. *J. Biol. Chem.* 274:21797–21803.

Hatzfeld, M., and K. Weber. 1990. Tailless keratins assemble into regular intermediate filaments in vitro. *J. Cell Sci.* 97:317–324.

Herrmann, H., and U. Aebi. 1998. Structure, assembly, and dynamics, of intermediate filaments. *In* Subcellular Biochemistry Vol. 31: Intermediate Filaments. H. Herrmann, and J.R. Harris, editors. 319–355.

Hesse, M., T.M. Magin, and K. Weber. 2001. Genes for intermediate filament proteins and the draft sequence of the human genome: Novel keratin genes and a surprisingly high number of pseudogenes related to keratin genes 8 and 18. *J. Cell Sci.* 114:2569–2575.

Jones, J.M., K. Nau, M.T. Geraghty, R. Erdmann, and S.J. Gould. 1999. Identification of peroxisomal acyl-CoA thioesterases in yeast and humans. *J. Biol. Chem.* 274:9216–9223.

Lu, X., and E.B. Lane. 1990. Retrovirus-mediated transgenic keratin expression in cultured fibroblasts: specific domain functions in keratin stabilization and filament formation. *Cell.* 62:681–696.

Ma, L., S. Yamada, D. Wirtz, and P.A. Coulombe. 2001. A "hot-spot" mutation alters the mechanical properties of keratin filament networks. *Nat. Cell Biol.* 3:503–506.

Mack, J.W., A.C. Steven, and P.M. Steinert. 1993. The mechanism of interaction of filaggrin with intermediate filaments. The ionic zipper hypothesis. *J. Mol. Biol.* 232:50–66.

Marchuk, D., S. McCrohon, and E. Fuchs. 1984. Remarkable conservation of structure among intermediate filament genes. *Cell.* 39:491–498.

Matsudaira, P. 1994. The fimbrin and α-actinin footprint on actin. *J. Cell Biol.* 126:285–287.

Nikolic, B., E. MacNulty, B. Mir, and G. Wiche. 1996. Basic amino acid residue cluster within nuclear targeting sequence motif is essential for cytoplasmic plectin-vimentin network junctions. *J. Cell Biol.* 134:1455–1467.

Omary, M.B., N.-O. Ku, J. Liao, and D. Price. 1998. Keratin modifications and solubility properties in epithelial cells and in vitro. *In* Subcellular Biochemistry Vol. 31: Intermediate Filaments. H. Herrmann, and Harris, J.R., editors. 105–132.

Paladini, R.D., and P.A. Coulombe. 1999. The functional diversity of epidermal keratins revealed by the partial rescue of the keratin 14 null phenotype by keratin 16. *J. Cell Biol.* 146:1185–1201.

Paladini, R., K. Takahashi, T.M. Gant, and P.A. Coulombe. 1995. cDNA cloning and bacterial expression of the human type I keratin 16. *Biochem. Biophys. Res. Comm.* 215:517–523.

Pollard, T.D., and J.A. Cooper. 1982. Methods to characterize actin filament networks. *Meth. Enzymol.* 85:211–233.

Sprecher, E., A. Ishida-Yamamoto, O.M. Becker, L. Marekov, C.J. Miller, P.M. Steinert, K. Neldner, and G. Richard. 2001. Evidence for novel functions of the keratin tail emerging from a mutation causing ichthyosis hystrix. *J. Invest. Dermatol.* 116:511–519.

Stasiak, P.C., P.E. Purkis, I.M. Leigh, and E.B. Lane. 1989. Keratin 19: predicted amino acid sequence and broad tissue distribution suggest it evolved from keratinocyte keratins. *J. Invest. Dermatol.* 92:707–716.

Wawersik, M., and P.A. Coulombe. 2000. Forced expression of keratin 16 alters the adhesion, differentiation, and migration of mouse skin keratinocytes. *Mol. Biol. Cell.* 11:3315–3327.

Wilson, A.K., P.A. Coulombe, and E. Fuchs. 1992. The roles of K5 and K14 head, tail, and R/K L L E G E domains in keratin filament assembly in vitro. *J. Cell Biol.* 119:401–414.

Downloaded from http://rupress.org/jcb/article-pdf/155/5/747/1300632/jcb1555747.pdf by guest on 20 June 2021